

Analysis of residual stress and distortion

J Sivakumar^a Dr.G.R.Jinu^b D.Kumaresan^c

^a Student, M.E (CAD), University college of Engineering, Nagercoil – 629004

^b Asst. Professor, Dept. of Mechanical Engineering, University college of Engineering, Nagercoil

^c Research Scholar, Indian Institute of Science, Bangalore – 560012

Abstract

In this paper, cirseam welding (GTAW) of aluminum alloy tube is simulated. The temperature distribution in the girth welded joint of AA6061-T6 tube is evaluated. The finite element analysis of thermal distribution in single pass girth welding of two tubes is performed with ANSYS Software. This analysis includes a finite element model for thermal welding simulation. It also includes volumetric double ellipsoidal moving heat source, material deposit, temperature dependent material properties and transient heat transfer. The element birth and death technique is employed for simulation of filler metal depositions. The temperature distribution pattern and magnitude is obtained. This result is used for estimation of residual stress and distortion due to welding which are the major sources for weld crack. In order to avoid such weld crack, the thermal stress in weld joint has to be minimised by controlling weld heat input. The residual stress and distortion happened due to welding is also analysed using ANSYS.

1. Introduction

Welding is widely used in the fabrication of ships, oil-drilling rigs, pipe lines, space crafts, rockets, nuclear and pressure vessels. Welded structures are superior in many respects compared to riveted structures, castings and forging. Simulation of welding process is gaining importance these days, especially in the aerospace engineering community since this facilitates the failure prevention and optimisation of welded pressure vessels.

TIG welding or GTAW (Gas Tungsten Arc Welding) is one uses a non-consumable tungsten electrode protected by an inert gas. The electrical discharge generates a plasma arc between the electrode tip and the

work piece to be welded. The arc consists of a high-temperature conducting plasma that produces the thermal energy needed to melt the base and the filler material. The arc temperature spans between 12000 K and 15000 K above the pool surface and the temperature of the melted surface spans from 670 K to 1000 K, dependent on the material. Filler material in form of cold wire is fed in front of the melted pool. The filler material is usually the same as the base material. An inert gas is used to sustain the arc and to protect the melted pool and the electrode from atmospheric contamination. Depending on the welding parameters and welding materials, either argon, helium or a mix of the two gases can be used.

Aluminum is of interest mainly because of its low density. Aluminum alloys also have good fracture toughness at low temperatures, and they are antimagnetic. Some of the new aluminum alloys are competitive with some steels show a tendency toward lower notch toughness and questionable fatigue life. Pure aluminum can be readily alloyed with many other metals to produce a wide range of physical and mechanical properties.

Aluminium and aluminium alloys are usually welded using argon as inert gas. However, the addition of helium can be used to improve the heat transfer and is therefore sometimes used for the welding of thicker parts.

The four digit system of classifying aluminum alloys are used by the aluminum association.

1st digit = major constituents

2nd digit = the modification

3rd and 4th digits = alloy

In the 2xxx – 8xxx alloy classification group, the last two digits have no special significance, but are used to identify different aluminum alloys in the group.

Table 1
Major alloying elements in the wrought aluminum alloys

SL. NO.	Major alloying element	Designation
1	99.0% minimum Aluminum	1 xxx
2	Copper	2 xxx
3	Manganese	3 xxx
4	Silicon	4 xxx
5	Magnesium	5 xxx
6	Magnesium and silicon	6 xxx
7	Zinc	7 xxx
8	Other elements	8 xxx
9	Unused series	9 xxx

The 2xxx and 7xxx are called “aircraft alloys” and have high strength and are heat treatable.

Aluminium alloy AA6061 is taken up for this work which is an age hardenable wrought alloy and possesses excellent corrosion resistance, good machinability and good formability. This alloy can be clad with AA 7072 and the corrosion resistance is not significantly lowered by welding, but may be improved by cladding. This alloy is by far the most popular aluminium extrusion alloy and has excellent anodising characteristics. Typical applications of this alloy are found in trucks, towers, railroads, cars, furniture, pipelines and other structural applications where strength, weldability and corrosion resistance are needed.

Alloys are classified further into two broad categories: heat treatable and non-heat treatable. The first is stronger and more expensive because of the heat treatment involved. A letter following the alloy designation and separated from it by a hyphen indicates the basic temper designation. Those compositions that are hardenable only by strain hardening are given “H” designations; whereas those hardenable by heat treatment through precipitation or a combination of cold work and precipitation are given the letter “-T”.

A second numeral following the basic temper indicates the degree of hardness produced by the specific processing operation. In this work AA6061 alloy in T6 condition is taken up which represents ‘solution treated and artificially aged’.

Welding of aluminium alloys are challenging as the following problems occur:

- (a) Porosity in welds: compared with steel, aluminum alloys are much more active and thus are prone to weld porosity.
- (b) Shrinkage and distortion: Aluminum alloys compared with steel, have higher heat conductivity, larger thermal expansion coefficients and a lower modulus of elasticity. Therefore, welds in aluminum alloys have more shrinkage and distortion.
- (c) Loss of strength in the heat affected zone: A reduction in the strength of the heat affected zone has been experienced in weldments in aluminum alloys, especially heat treated alloys.

After welding operation the cooling of the molten is accompanied by shrinking in all the main directions. Residual strain and stress distributions coming from shrinking are largely influenced by the nature and configuration of the welding process, by metallurgical characteristics of weld and by the geometrical shape of the welded joint. Then this can lead to a crack occurrence, stress corrosion, deformation, loss of mechanical characteristics, and loss of interchangeability. So these residual stresses have to be known in order to get a better knowledge of the phenomenon to minimise the above risks. In this work, the process of welding is simulated by the FE method. The temperature and phase evolution are determined as a function of time in the thermal analysis. The temperature history of welded components has a significant influence on the residual stresses, distortion, and hence the fatigue behavior of welded structures.

Prediction of welding residual stresses is gaining importance these days, especially in the aerospace engineering community since this facilitates the failure prevention and optimization of welded pressure vessels.

In order to obtain a good prediction for residual stress and distortion in welded joints and structures, an accurate thermal model is to be created for that purpose. This work involves the thermal simulation of AA6061 T6 pipes girth welding process.

2. Thermal field

The objective with heat transfer analysis in welding applications is to determine the temperature fields in an object resulting from conditions imposed on its boundaries. The quantity that is sought is the temperature distribution, which represents how temperature varies within positions in the object. When this distribution is known, the conduction heat flux

calculated at any point in the medium or at the surface may be computed from Fourier's law.

The temperature fields during welding are highly heterogeneous and transient. The temperature of a component can vary from below zero to 3000 degree centigrade, i.e. the evaporation temperature of the metal. Within this range phase changes, micro structural transformations and thermal strains take place, all of which determine residual stresses and distortion. Fourier's law of heat conduction describes the heat propagation in mechanism in the solid material. The law states that the heat flow density q [J/mm^2] is proportional to the negative temperature gradient.

$$q = -\lambda \frac{\partial T}{\partial n} \quad (2.1)$$

Where, λ [$J/mm \cdot s \cdot K$] denotes the thermal conductivity and

T [K] the temperature. Consider a homogenous medium expressed in one dimension x with a temperature distribution (T_x) expressed in Cartesian coordinates with infinitesimally small control volume dx . The condition heat rate at the control area can then be expressed as q_x . The condition heat rate at the opposite surface can be expressed as a Taylor series expansion neglecting higher order terms as

$$q_{x+dx} = q + \frac{\partial q_x}{\partial x} dx \quad (2.2)$$

Inside the control medium an energy source term (2.3) and an energy storage term (2.4) can be expressed as

$$\dot{E}_g = \dot{q} dx \quad (2.3)$$

$$\dot{E}_s = \rho C_p \frac{\partial T}{\partial t} dx \quad (2.4)$$

Using the law of energy conservation equations 2.1, 2.3 and 2.4 can be substituted to

$$q_x + \dot{q} dx - q_{x-dx} = \rho C_p \frac{\partial T}{\partial t} dx \quad (2.5)$$

Substitution from equation 2.2 and Fourier's law the heat diffusion equation can be written in a general form, in three dimensional Cartesian coordinates as,

$$\frac{\partial}{\partial x} \left[\lambda(T) \frac{\partial T}{\partial x} \right] + \frac{\partial}{\partial y} \left[\lambda(T) \frac{\partial T}{\partial y} \right] + \frac{\partial}{\partial z} \left[\lambda(T) \frac{\partial T}{\partial z} \right] = \rho C_p (T) \frac{\partial T}{\partial t} - Q \quad (2.6)$$

Where, the Cartesian coordinates x , y and z denote the welding direction, the transverse direction, and the normal direction to the weld melt surface, respectively, Q [W/mm^3] stands for internal heat generation rate and the material properties, thermal conductivity, density, and specific heat, are denoted by λ , ρ and C_p respectively.

Several possibilities for initial conditions exist. The most common is: $T = T_0$ at $t=0$

A general boundary condition can be written as:

$$\lambda \frac{\partial T}{\partial x} l_x + \lambda \frac{\partial T}{\partial y} l_y + \lambda \frac{\partial T}{\partial z} l_z - \dot{q} + h(T - T_\infty) = 0 \quad (2.7)$$

where h denotes surface heat loss coefficient, $x l$, $y l$ and $z l$ the direction cosines to the boundary surface. The surface temperature and environment temperature are denoted T and T_∞ respectively.

The heat diffusion equation (2.6) can be solved both analytically and numerically (in the latter case, the FEM is commonly used).

The equation can be analytically solved assuming the following conditions:

- The energy from the welding heat source is applied at a uniform rate.
- The heat source is moving with a constant speed.
- The cross section of the work piece is constant.
- Constant material properties are used.

3. Heat source model

In order to obtain a good prediction in welded joints, an appropriate heat source is needed for that purpose. Energy was deposited using a volumetric heat source. A circular shape was used on the surface of the part. An ellipsoidal shape was used for the heat source in the thickness section of the weld. The heat source distribution was assumed to be Gaussian in all directions (depth, axial, and circumferential). Heat source dimensions were half the weld width on the surface of the pipe. The heat source depth equaled the part thickness.

Goldak et al. proposed a model with a double ellipsoidal moving heat source configuration to incorporate this volume heating and the size and shape of the heat source can be easily changed to model both the shallow and deep penetrating welding processes. In addition, it has the versatility and flexibility to handle non-axis-symmetric cases such as strip electrodes or dissimilar metal joining. Goldak initially proposed a

semi-ellipsoidal heat source in which heat flux was distributed in a Gaussian manner throughout the heat source's volume. This heat source predicted the temperature

gradients in front of the arc is less steep than experimentally observed and steeper behind the arc. A double ellipsoidal heat source was proposed to overcome that problem and the same model is employed in the present paper to model heat input from the welding torch. Goldak double ellipsoidal heat source model is shown at Figure 1. The front half of the source model is the quadrant of one ellipsoid, and the rear half is the quadrant of another ellipsoid. The specific mathematical expression is shown as follows.

The power density distribution of the front half is shown at Equation 3.1.

$$q(x, y, z) = \frac{6\sqrt{3}\eta Q_f}{a_f b c \pi \sqrt{\pi}} e^{-\left(\frac{3x^2}{b^2} + \frac{3y^2}{c^2} + \frac{3z^2}{a_f^2}\right)} \quad (3.1)$$

Similarly, the power density distribution of the rear half is shown at Equation 3.2.

$$q(x, y, z) = \frac{6\sqrt{3}\eta Q_r}{a_r b c \pi \sqrt{\pi}} e^{-\left(\frac{3x^2}{b^2} + \frac{3y^2}{c^2} + \frac{3z^2}{a_r^2}\right)} \quad (3.2)$$

Where, $Q = VI$ and $f_f + f_r = 2$

Where a_f, a_r, b, c are the shape parameters, q_o is effective heat input, f_f and f_r are the fractions of the heat deposited in the front and rear half, all are heat input parameters. The $6\sqrt{3}\eta$ is heat flux distribution parameter actually, characterize the concentration level of heat flux distribution, based on the heat flux concentration level or heat flux distribution feature of a welding method to determine its value. The shape of the volume in which the power is distributed can be chosen by varying the parameters a_f, a_r, b and c . In this way, experimental fusion zone geometry can be approached. Data for weld pool geometries can be obtained from experiments. If such data are not available, the methods for estimating the weld pool dimensions (for arc welding) suggested by Goldak et al. report good agreement between actual and modeled weld pool sizes, if the modeled heat source size is selected approximately 10% smaller than the experimental weld pool size. Also, in the absence of better data, the distance in front of the heat source equal one half the weld widths and the distance behind the heat source equal to twice the width gives better approximations.

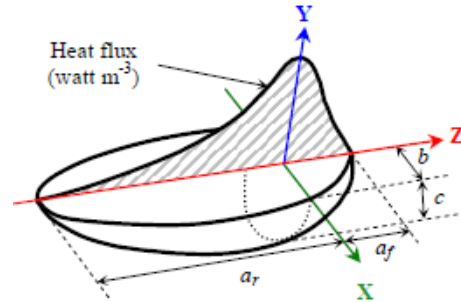


Fig.1 Goldak's double ellipsoid heat source model for welding heat source

4. Welding simulation

The welding process of a butt-weld joint of two AA6061 aluminium alloy tubes of $\varnothing 66$ mm and 3 mm thickness was simulated. Due to high temperature and stress gradients near the weld, the finite element model has a relatively fine mesh in both sides of the weld center line. The eight-node brick elements with linear shape functions are used in meshing the model. To simulate the moving heat source it is necessary to model the heat source during each time increment. In this analysis the moving heat source is simplified by assuming the welding arc stayed at an element with a constant specific volume heat generation, and then moved to the next element at the end of the load step as the welding was finished. The element type SOLID70, which has a single degree of freedom, was used for the thermal analysis.

The heat transfer analysis requires thermal conductivity, specific heat, density (constant) and combined convection and radiation heat coefficient. Thermal conductivity gives a measure of the ease of heat flow through a material.

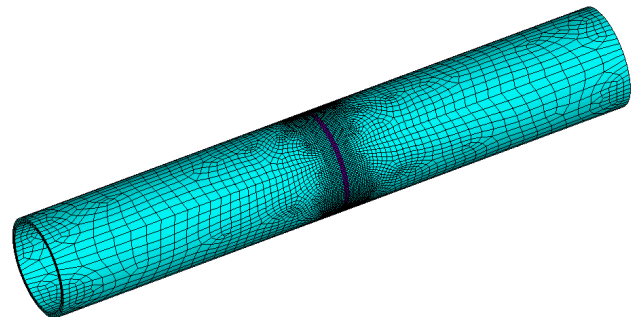


Fig.2. Expanded FE model of pipe for welding simulation

To simplify the heat transfer analysis, the following assumptions were made.

- All boundaries were assumed to satisfy the adiabatic condition.
- The portion underneath the arc was assumed to be insulated during the time the arc was applying to the surface.
- A combined convection and radiation boundary condition was used on the remaining of the top surface. The formula is as follows:

$$H = 24.1 \times 10^{-4} \xi T^{1.61}$$

Where, H is the combined convection and radiation heat transfer coefficient. ξ is thermal emissivity, and T is the temperature.

- The analysis is based on quasi-steady state, i.e., the heat source is moving at a constant velocity.
- The moving heat source was modeled based on double ellipsoid heat source distribution.

Table 2
Material properties of AA6061 T6 alloy

Density kg/m ³	Elastic Modulus E (GPa)	Thermal properties			ρ $\mu\Omega$ m
		K W/m K	C _P J/kg K	α $\times 10^{-6}$ K ⁻¹	
2700	68.3	167	0.896	23.60	0.040

4.1 Parameters taken for simulation

The heat input during welding is modeled in the ANSYS by the equivalent heat input which includes body heat flux.

The amount of heat input was calculated as follows:

$$Q = \eta \frac{UI}{V} \quad (4.1)$$

where: η is arc efficiency, V is the travel speed, U and I are the arc voltage and the current, respectively. In this analysis, the current was 70A, the voltage was 16V and the welding speed was 0.86 mm/sec, while the arc efficiency of the process considered to be 70%.

A local coordinate was placed at the starting point of the weld line. The local coordinate is moved along the weld line so as to simulate the moving weld source. As the source reaches the other end the heat source is removed and the cooling take place due to convection. Post processing is done to get the required result.

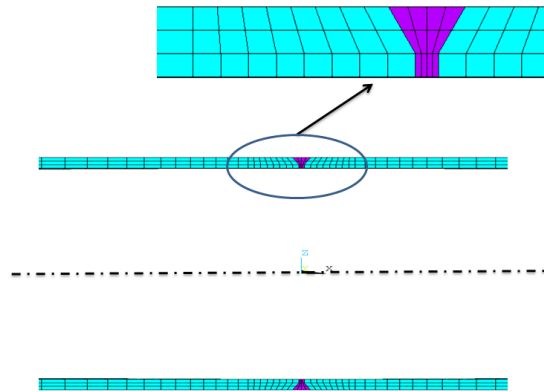


Fig.3 Cross section of FE model

4.2 Material addition

So as effectively simulate the bead on pipe welding process and to study the penetration effects it is required to bring in the concept of material addition which is achieved by means of element birth and death feature available in ANSYS. In this present model a 8 mm wide, 0.5 mm thick layer of bead is modeled. The property of bead material is also given as a function of temperature.

4.3 “Birth and Death” Feature

The material deposition is modeled using an element “birth and death” technique. To achieve the “death element” effect, the ANSYS code does not actually remove the element from the model. Instead, the weld elements are first deactivated by multiplying their stiffness (or conductivity, or other analogous quantity) by a huge reduction factor. Meanwhile, to obtain the “birth element” effect, the ANSYS program then reactivates the “death element” by allowing its stiffness, mass, element loads, etc. return to their original values.

In this analysis material deposition is studied for calculating the weld penetration.

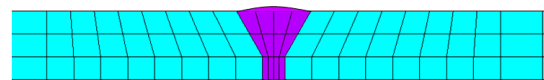


Fig.4 Model for Material Addition

From the model developed similar heat transfer analysis was carried out and the concept of material addition was incorporated using element birth and death principle.

5. Residual stress & distortion analysis

Coupled field analysis was carried out to obtain the distortion and residual stress by mapping of thermal load on structural nodes. The element type used for structural analysis is SOLID 45 which is used for the 3-D modeling of solid structures. The element is defined by eight nodes having three degrees of freedom at each node. Temperatures and fluences may be input as element body loads at the nodes in this element type.

6. Results & Discussion

The girth welding of AA6061 T6 pipes of size Ø66x3 is thus modeled with pre-heating at constant welding heat input and velocity. Post processing is done to interpret the results.

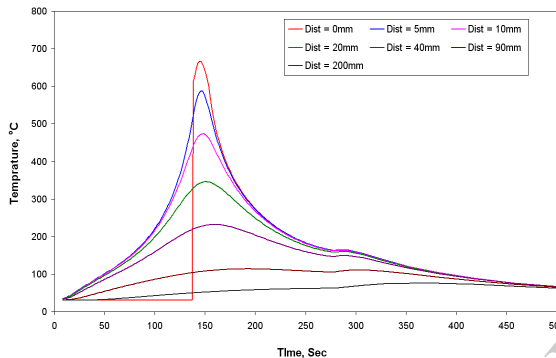


Fig.5 Transient temperature distribution at different location from the weld-bead

Fig.5 shows the temperature plot at various distances from the weld and also on the line of weld. Distance '0 mm' is at 180° from start point of weld. Since there is no material available at joint portion before weld, the temperature at this point is maintained at room temperature till the weld arc reaches that point. The phenomenon of reduction in temperatures at locations away from the weld due to heat dissipation is thus simulated.

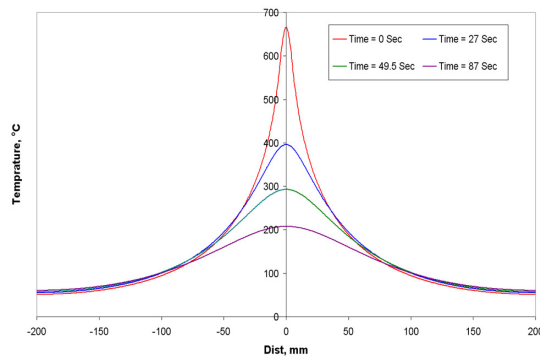


Fig.6 Temperature distribution on various time instant(perpendicular to weld direction)

Figure 6 shows the variation of temperature distribution perpendicular to the weld zone at various time intervals. This temperature distribution result is used to get the heat input required for the residual stresses estimation.

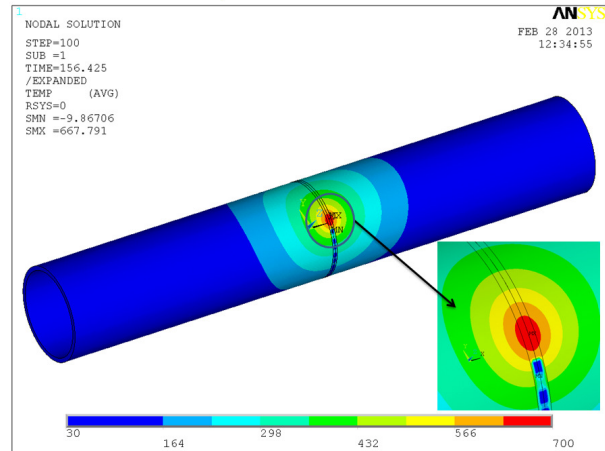


Fig.7 Temperature distribution result

Figure 7 shows the temperature distribution result. A maximum of 700 degree Celsius is noticed in weld arc zone and the temperature distribution along the axis of tube is also obtained. This distribution is used to predict the thermal load.

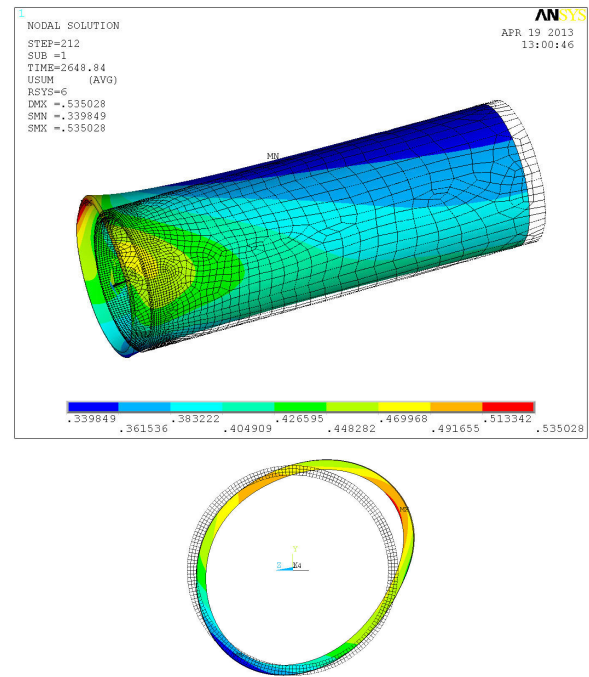


Fig.8 Distortion contour plot

Fig.8 shows the maximum residual deformation i.e. distortion in radial direction. It is evaluated as 0.535 mm at around 135° from start of weld.

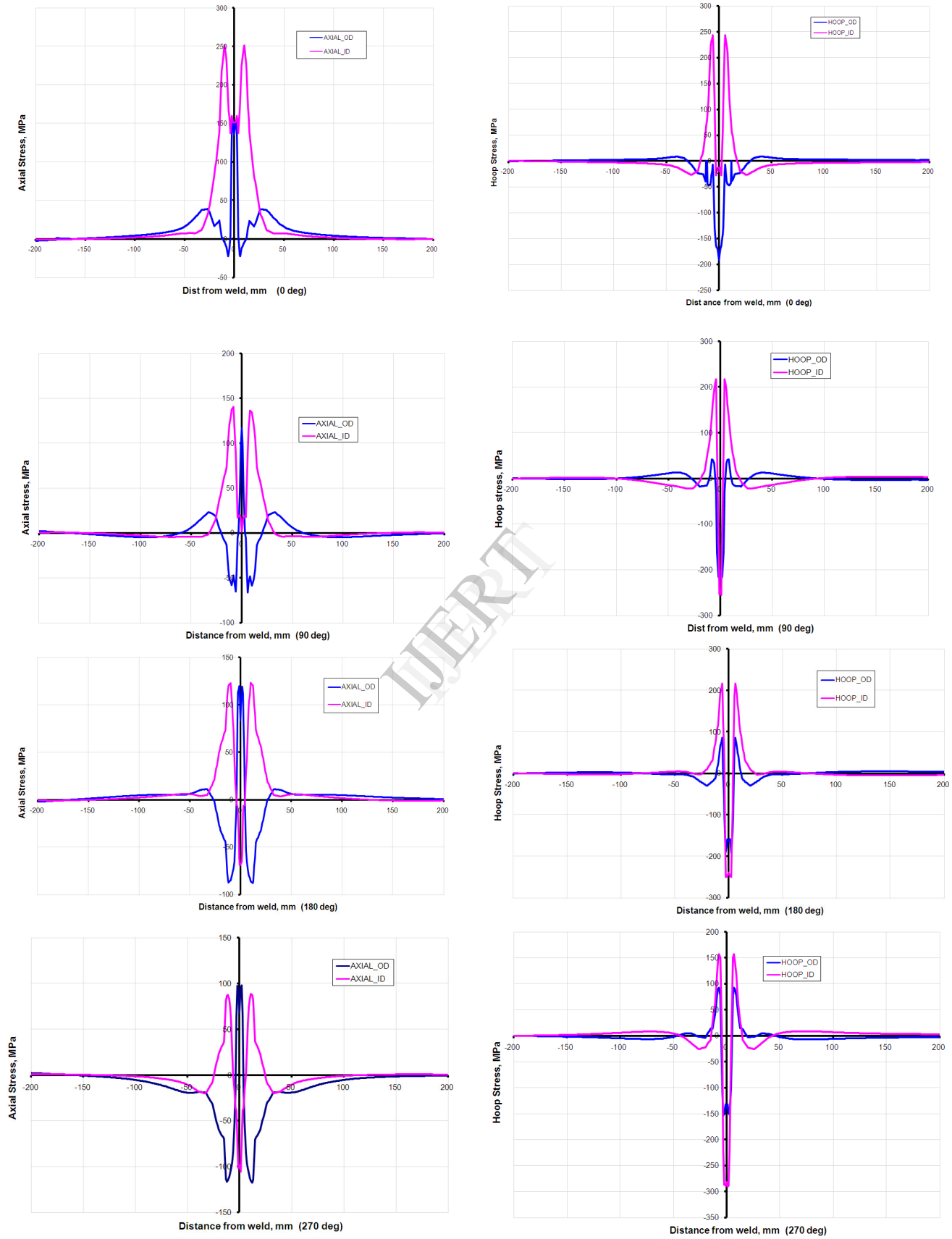


Fig.9 Results of residual axial and hoop stress at 0, 90, 180 & 270 degree angles from start of weld w.r.t. axial distance from weld

Fig.9 shows the variation of residual axial stress and residual hoop stress with respect to distance at various angles. It is found that the axial stress is tensile in ID and compressive in OD except near 0 deg. This is due to un-symmetrical loading at the solidification and termination of heat source model with respect to time at 0 degree. The difference in stress at OD and ID causes bending stress.

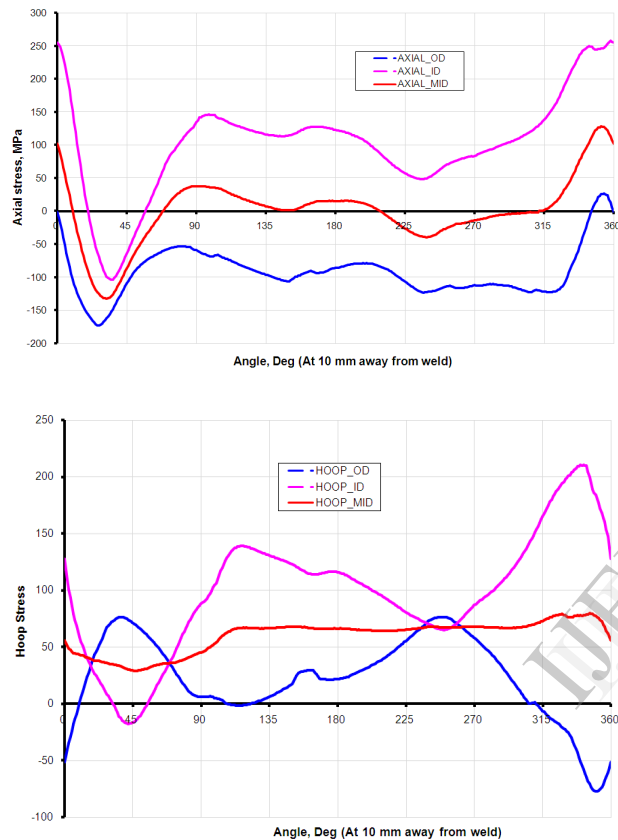


Fig.10 Residual stress at 10 mm away from weld around the circumference

Fig.10 shows the maximum hoop and axial residual stress. The maximum residual stresses obtained in pipe ID is 250 Mpa whereas in OD the maximum residual stress is -120 Mpa at around 10mm away from weld.

In this paper, simulations of the welding process for butt joint using finite element analyses are presented. The base metal is aluminum alloy AA6061 – T6. The simulations are performed with the commercial software ANSYS, which includes moving heat sources, material deposit, metallurgy of binary aluminum, temperature dependent material properties, transient heat transfer and mechanical analyses. One-way thermo-mechanical coupling is done, which means that the thermal analysis is completed first, followed by a

separate mechanical analysis based on the thermal history to evaluate residual stress and distortion.

7. Conclusion

- 1) The heat source was developed for the simulation purpose.
- 2) The double ellipsoid model has been used to study penetration and heat affected zone characteristics.
- 3) Simulation is very sensitive to parameters like efficiency (η), distribution parameters (a, b and c). To obtain more accurate predictions these parameters are to be simulated as far as possible to the experimental values.
- 4) The temperature distribution obtained from this simulation is used for computation of the residual stresses and distortion by coupled field analysis.
- 5) It is inferred from the structural analysis, the axial residual stress varies with respect to angle. This is due to unsymmetrical loading of heat source. Hence, this paper recommends to carry out the welding simulation using 3D model with moving heat source.

8. References

- [1] Goldak, J., Bibby, M., Moore, J., House, R., and Patel, B. 1986 "Computer modeling of heat flows in welds", *Metallurgical Transactions* 17B: 587–600.
- [2] Li Yajiang, Wang Juan, Chen Maoai And Shen Xiaoqin, "Finite element analysis of residual stress in the welded zone of a high strength steel", *Bull. Mater. Sci.*, Vol. 27, No. 2, April 2004, pp. 127–132. © Indian Academy of Sciences.
- [3] Dragi Stamenković, MSc (Eng), Ivana Vasović, BSc (Eng), "Finite Element Analysis of Residual Stress in Butt Welding Two Similar Plates," *Scientific Technical Review*, Vol.LIX, No.1, 2009.
- [4] Muhammad ejaz qureshi, "Analysis of residual stresses and distortions in circumferentially welded thin-walled cylinders," *Department of Mechanical Engineering, College of Electrical and Mechanical Engineering, National University of Sciences and Technology, Rawalpindi, Pakistan, Year 2008*
- [5] M Jeyakumar, T Christopher, R Narayanan & B Nageswara Rao, "Residual stress evaluation in butt-welded steel plates", *Indian Journal of Engineering & Materials Sciences* Vol. 18, December 2011, pp. 425-434